의학박사 학위논문

Biomechanical analysis of lumbar decompression surgery in relation to degenerative changes in the lumbar spine - Validated finite element analysis

유한요소모델을 이용한 요추의 퇴행성 변화에 따른 요추 감압술 이후 추간판의 생역학적 변화 분석

2018년 8월

서울대학교 대학원
의과대학 의학과
LI QUANYOU

Biomechanical analysis of lumbar decompression surgery in relation to degenerative changes in the lumbar spine - Validated finite element analysis

지도교수 염 진 섭

이 논문을 의학과 박사학위논문으로 제출함
2018년 7월

서울대학교 대학원
의과대학 의학과 전공
LI QUANYOU

LI QUANYOU의 박사학위논문을 인준함
2018년 7월

위 원 장 _____ **(인)**
부위원장 _____ **(인)**
위 원 _____ **(인)**
위 원 _____ **(인)**
위 원 _____ **(인)**

Abstract

Background : There are no studies about the biomechanical analysis of lumbar decompression surgery in relation to degenerative changes of the lumbar spine. Therefore, the purpose of this study was to compare, by using finite element (FE) analysis, the biomechanical changes of the lumbar spine in terms of annulus stress and nucleus pressure after two different kinds of lumbar decompression surgery in relation to disc degenerative changes.

Methods : The validated intact and degenerated FE models (L2-5) were used in this study. In these two models, two different decompression surgical scenarios at L3-4, including conventional laminectomy (ConLa) and the spinous process osteotomy (SpinO), were simulated. Therefore, a total of six models were simulated. Under preloading, 7.5 Nm moments of flexion, extension, lateral bending, and torsion were imposed. In each model, the maximal von Mises stress on the annulus fibrosus and nucleus pressure at the index segment (L3-4) and adjacent segments

(L2-3 and L4-5) were analyzed.

Results : The ConLa model and disc degeneration model demonstrated a larger annulus stress at the decompression level (L3-4) under all four moments than were seen in the SpinO model and healthy disc model, respectively. Therefore, the ConLa model with moderate disc degeneration showed the highest annulus stress at the decompression level (L3-4). However, the percent change of annulus stress at L3-4 from the intact model to the matched decompression model was less in the moderate disc degeneration model than in the healthy disc model.

Conclusions : Although the ConLa model with moderate disc degeneration showed the highest annulus stress, the degenerative models would be less influenced by the decompression technique.

Keywords : lumbar spine, decompression surgery, degenerative changes, laminectomy, spinous process osteotomy, finite element model

Student Number : 2013-30812

Table of Contents

Chapter 1. Introduction

Several surgical treatments have been introduced for decompression of lumbar spinal stenosis (LSS), ranging from minimally invasive techniques to traditional laminectomy. Previous studies have shown that decompression surgery alters the biomechanical behavior of the lumbar spine.[1,2] Especially, preservation of the continuity of the posterior ligament complex (PLC) is important in alleviating instability after decompression surgery.[2]

Degenerative changes of the lumbar spine also influence spine biomechanics.[3-5] Given that all patients with LSS have moderate to severe degenerative changes, the effect of this degeneration should be considered for the proper and valid prediction of biomechanical changes after decompression surgery. The removal of posterior structures for sufficient decompression might have different biomechanical implications depending on the degenerative state of the lumbar spine at the time of surgery.

Although both decompression surgery and degenerative changes can influence the biomechanics of the lumbar spine, there has been no study about a simultaneous biomechanical effect of decompression surgery and degenerative changes. Therefore, we hypothesized that biomechanical effect of decompression surgery would be different in relation with degenerative changes. The information about this would be clinically relevant because this may help the surgeon decide surgical method for degenerative spinal disease. Therefore, this study aimed to assess and compare, by using finite element (FE) analysis, the biomechanical changes of the lumbar spine for annulus stress and nucleus pressure after two different kinds of lumbar decompression surgery in relation to degenerative changes of the lumbar spine. Two different surgical decompression techniques were compared: the spinous process osteotomy (SpinO) technique, which preserves the PLC but involves the cutting of the base of the posterior spinous processes, and conventional laminectomy (ConLa), which involves the removal of both

the PLC and the spinous processes.

Chapter 2. Materials and Methods

2.1. FE model of the intact lumbar spine (L2-5)

We made a three-dimensional (3D) nonlinear FE model of the lumbar spine comprising four lumbar vertebrae, three intervertebral discs, and the associated spinal ligaments. The geometric outline of the human lumbar spine (L2-L5) was obtained from high-resolution computed tomography (CT) images of a 46-year-old male subject with no spinal deformities. Although we obtained anatomical information about the lumbar spine geometry from CT images, a large part of the geography was altered for specific use in this study. With the respect to mid-sagittal plane, the geometry was modified to be symmetric. In addition, because it was difficult to distinguish geometry of the disc nucleus from the CT image, it was modeled based on the previous literature.[6-7] Similarly, cortical and cancellous bone were also modeled on the basis of the method from the previous studies.[6-7] Furthermore, because the pre-

sent research used existing data and the subjects could not be identified, our institutional review board approved an exemption for obtaining informed consent in this study. Digital CT data were imported to a software program (Mimics; Materialise Inc., Leuven, Belgium) that was used to generate the 3D geometric surface of the lumbar spine. Initial Graphic Exchange Specification files exported from the Mimics software were input into Unigraphics NX 3.0 (Siemens PLM Software, Torrance, CA, USA) to form solid models for each vertebral segment. The solid model was then imported into Hypermesh 8.0 (Altair Engineering Inc., Troy, MI, USA) to generate FE meshes. In the current FE model, a hexa mesh was generated over the entire area. The FE model was analyzed with commercially available software (ABAQUS 6.11–1; Hibbitt, Karlsson and Sorenson Inc., Providence, RI, USA).

Three-dimensional solid elements with homogenous and transversely isotropic character were used to model the cortical and cancellous cores and the posterior bony parts of the vertebrae. The nucleus pulposus

(NP) and the ground substance of the annulus fibrosus (AF) were modeled by using solid elements. The anterior longitudinal ligament, posterior lon- gitudinal ligament, intertransverse ligament, ligamentum flavum, capsular ligament, interspinous ligament, and supraspinous ligament were modeled by using tension-only truss elements (Fig. 1).

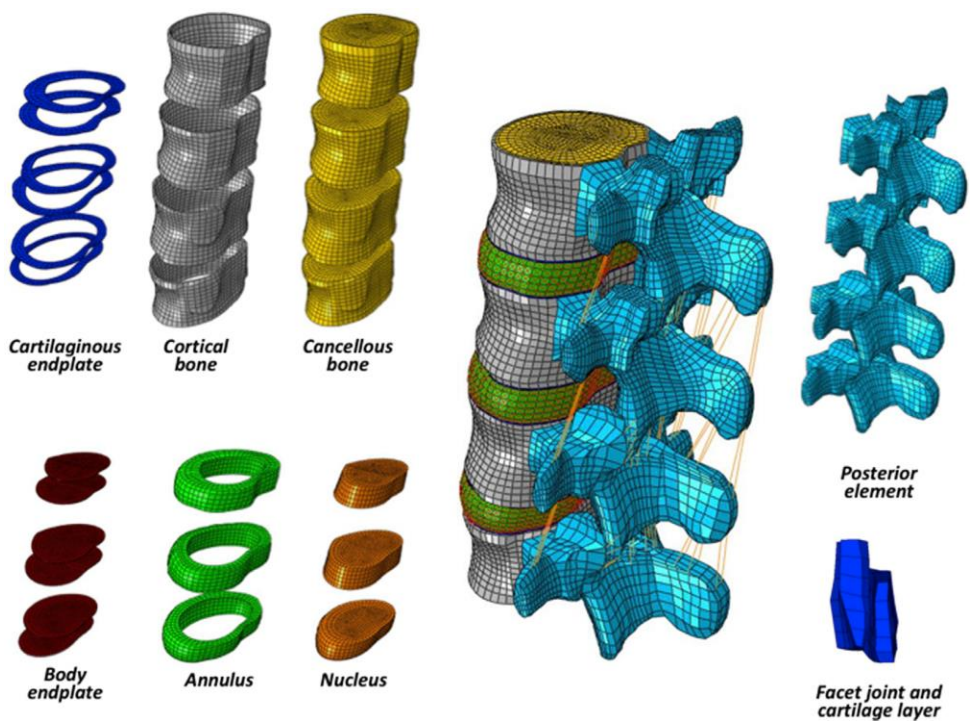

Fig. 1. The present intact finite element model.

2.2. Material properties

The material properties were derived from various literature sources (Table 1).[8-11] The cortical and cancellous regions of the vertebrae were modeled independently. Because the cortical and trabecular bones in the posterior region were difficult to differentiate from each other, the posterior elements were all assigned a single set of material properties. The AF was modeled as a composite of a solid matrix with embedded fibers (by using the REBAR parameter) in concentric rings surrounding an NP, which was considered to be an incompressible solid. Element members with a hybrid formulation (C3D8H) combined with a low elastic modulus and large Poisson ratio definitions were applied to simulate the NP. A hybrid formulation (C3D8H) was also applied for simulation of ground substance of AF. Eight-node brick elements were used to model the matrix of the ground substance. Each of the four concentric rings of the ground substance contained two evenly spaced layers of annulus fibers oriented at ±30°, relative to the horizontal plane. The

reinforcement structures of the annulus fibers were represented by truss elements with modified tension-only elasticity. In the radial direction, four double cross-linked fiber layers were defined. Those fibers were bounded by the annulus ground substance and both endplates. In addition, the elastic strength of these fibers proportionally decreases from the outermost (550 MPa) to the innermost (385 MPa) layer.[12,13]

The articulating facet joint surfaces were modeled by using surface-to-surface contact elements in combination with the penalty algorithm with a normal contact stiffness value of 200 N/mm and a friction coefficient of zero. The thickness of the cartilage layer of the facet joint was assumed to be 0.2 mm. The initial gap between the cartilage layers was assumed to be 0.5 mm. The cartilage was assumed to be isotropic and linearly elastic, with a Young's modulus of 35 MPa and a Poisson's ratio of 0.4.[14] Spinal ligaments were represented with nonlinear material properties. The naturally occurring changes in the ligament stiffness (initially low stiffness at low strains, followed by increasing stiffness at

higher strains) were simulated through a bilinear material designation (Table 1).

Table 1. Material properties in the present FE models

Component	Young's modulus (MPa)	Cross-section (mm2)	Poisson's ratio
Cortical bone	E_x = 11300 E_y = 11300 E_z = 22000 G_x = 3800 G_y = 5400 G_z = 5400		υ_{xy} = 0.484 υ_{xz} = 0.203 υ_{yz} = 0.203
Cancellous bone	E_x = 140 E_y = 140 E_z = 200 G_x = 48.3 G_y = 48.3 G_z = 48.3		υ_{xy} = 0.45 υ_{xz} = 0.315 υ_{yz} = 0.315
Posterior elements	3500		0.25

Disc			
Nucleus pulposus	Refer to Table 2		
Annulus (ground substance)	Refer to Table 2		
Annulus fiber	385 – 550		
Outermost	550	0.70	
Second	495	0.63	
Third	440	0.55	
Fourth	420	0.49	
Fifth	385	0.41	
Cartilaginous endplate	24.0		0.40
Cartilage layer of facet joint	35		0.4
Ligaments			
Anterior longitudinal	7.8(<12%) 20(>12%)	63.7	
Posterior longitudinal	10(<11%) 20(>11%)	20.0	
Ligamentum flavum	15(<6.2%) 19.5(>6.2%)	40.0	
Capsular	7.5(<25%) 32.9(>25%)	30.0	
Interspinous	10(<14%) 11.6(>14%)	40.0	
Supraspinous	8.0 (<20%) 15(>20%)	30.0	
Intertransverse	10(<18%) 58.7(>18%)	1.8	

Three-dimensional truss elements were used to simulate ligaments, which were active only with tension (Fig. 1).

2.3. Modeling of disc degeneration

A healthy model was modified to simulate a model of moderate degeneration at the L3-L4, and L4-L5 lumbar segments (Fig. 2). Degeneration was simulated by decreasing the disc height and nucleus area, and by modifying the material properties of the annulus ground substance and the NP. The disc height was reduced by 40% for the moderate disc degeneration models (Table 2) (Fig. 2).[15]

Table 2. Material properties for annulus ground substance and nucleus for healthy and moderate degeneration.

	Annulus ground substance			Nucleus pulposus			Disc height (mm)	
	Hyper-elastic Mooney–Rivlin		Area (mm^2) (L3-4 /L4-5) in mid-plane	Young's Modulus (MPa)	Poisson's ratio	Area (mm^2) (L3-4 /L4-5) in mid-plane	Anterior (L3-4/L4-5)	Posterior (L3-4 /L4-5)
	C1	C2						
Healthy	0.2	0.05	787 / 802	1.0	0.49	636/653	13.8 / 14.5	10.1 / 7.8
Moderate	0.9	0.23	1044 / 1103	1.66	0.4	379/352	8.3 / 8.7	6.1 / 4.7

This value was assumed on the basis of the grading schemes of a previous study.[16] The nucleus area was reduced according to the stress profilometry studies of Adams et al.[17] The decreased nucleus area was replaced with elements representing the annulus ground substance so as to maintain the same disc area. Therefore, disc height decreases and the cross-sectional area of ground substance of annulus increased with disc degeneration. Material properties were taken from the literature or linearly interpolated for moderate degeneration[3,15,18,19] (Table 2).

2.4. Simulation of decompression models

To simulate the SpinO model, the spinous processes of L3 and L4 were osteotomized at their bases in the model of the intact spine (L2-L5), whereas the interspinous ligaments and supraspinous ligaments between L3 and L4 were left intact. Then, decompression procedure was simulated as following. First, partial laminectomy was simulated by removal of inferior one-third of lamina. Second, the ligamentum flavum

underneath L3-4 lamina was removed. Third, partial facetectomy was simulated by removal of medical one third of facet joint (Fig. 3). This technique minimized the damage to the PLC.[20,21] To simulate the ConLa model, the distal half of the L3 spinous process was cut along with the supraspinous and interspinous ligaments between L3 and L4. This was followed by decompression procedures which was the same to that in the SpinO model, including partial laminectomy, removal of the ligamentum flavum of L3-4, and partial facetectomy (Fig. 3).

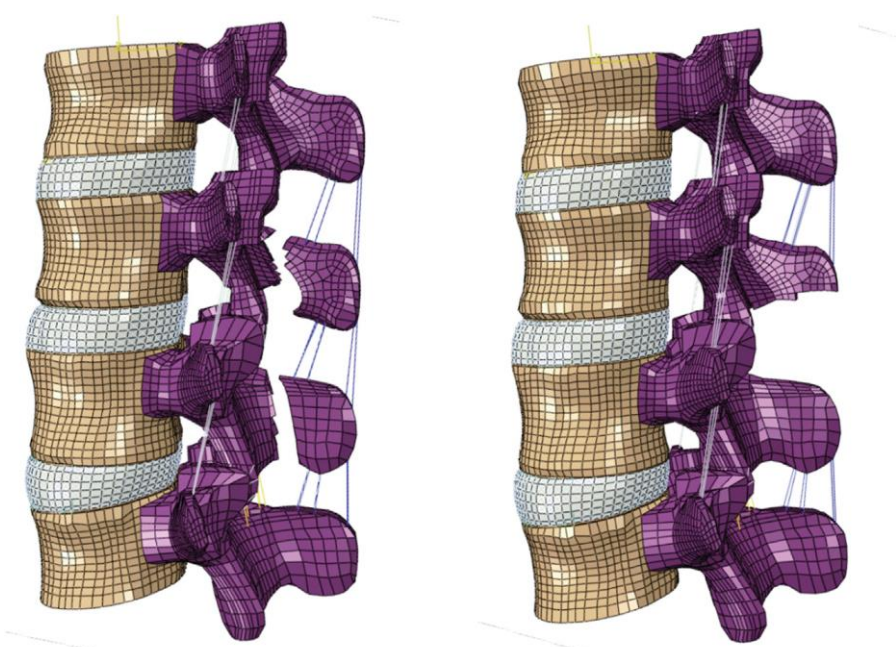

a. SpinO model　　b. ConLa model

Fig. 3. Finite element models with decompression surgery. a. Spinous process osteotomy model (SpinO), b. Conventional laminectomy model (ConLa).

2.5. Boundary and loading conditions

Previously validated intact lumbar models with healthy and moderate disc degeneration were used in this study.[22] For model validation, the biomechanical behaviors of the FE model (range of motion, intradiscal pressure, and facet contact force) were compared between the current FE study and previous experimental studies.[23-26] The experimental and simulated loading protocols were identical. For four pure moments, the range of motion results were compared with those of previous in vitro studies by Hartmann et al.[26] and Wilke et al.[23] The intradiscal pressure of the current model was compared with those in an experimental study by Schilling et al.[24] The facet contact force in our model was compared with that in a cadaver study by Wilson

et al.[25] For further validation of the healthy and degeneration models, the range of motion at the L3-4 segment in the present models were compared with those of previous studies by Mimura et al. and Rohlmann et al.[27,28] Furthermore, the results of annulus stress in the degeneration FE model were compared with those reported by Rohlmann et al.[28] More detailed validation methods were described in a previous study.[22] The second type of loading condition was the load control protocol. The follower load technique was used to simulate the vector sum of trunk muscle co-activation by a single internal force vector that acts tangentially to the curvature of the spine passing through each segmental center of rotation.[29] This "follower" path, tangential to the curvature of the spine, mimics physiologically relevant compressive loads on the lumbar spine, as seen in vivo. The 400 N compressive follower loads were simulated at each motion segment in the model by using a pair of two-node thermo-isotropic truss elements. The trusses were attached bilaterally to the cortical shell of the vertebrae at each motion

segment. Each truss spanned the disc space passing through the instantaneous center of rotation at each motion segment.[30] This load control protocol involved the application of 7.5 Nm flexion, extension, torsion, and lateral bending pure moments to three lumbar models on the L2 vertebral body under a 400 N follower load (Fig. 4).

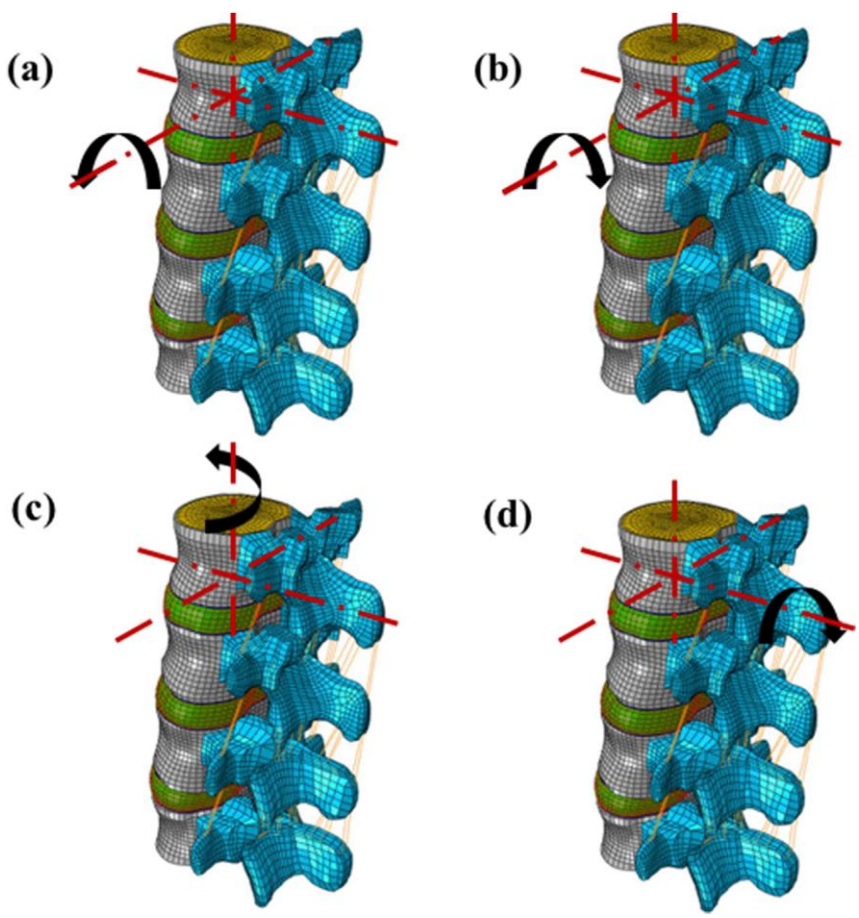

Fig. 4. Loading conditions. a. Flexion moment, b. Extension moment,

c. Torsion moment, d. Lateral bending moment.

To evaluate biomechanical effects of degenerative changes and decompression surgery, von Mises stress of annulus and disc pressure of nucleus were compared among the present models under above loading conditions. The von Mises stress is non-directional scalar and it is the effective criterion with a single value independent to maximum or minimum principle stress. The increase of von Mises stress means that the deformation energy on annulus becomes larger throughout the overall stress distribution on annulus.

Chapter 3. Results

3.1. Model convergence test and model validation

The current healthy and degeneration models have been validated in were used.[23-27] The calculated intersegmental rotations of the current healthy and degenerated FE models were within one standard deviation of the average values measured by Mimura et al. and Rohlmann et al.[27,28] Furthermore, the results of annulus stress in the present FE models predicted the same trends as those in the study by Rohlmann et al.[28]

3.2. Comparison of maximal von Mises stress in the annulus stress of the intact, SpinO, and ConLa models related to disc degeneration under four moments

The main difference of annulus stress among the three models was noted at the decompression level (L3-4) under exion moments. Compared with an annulus stress of 0.87 MPa at L3-4 under exion

moments in the intact healthy model, annulus stresses of 1.36 and 1.72 MPa were noted at the compression level (L3-4) under exion moments in the healthy SpinO and ConLa models, respectively. In addition, each degenerated SpinO and ConLa model showed an annulus stress of 2.20 and 2.76 MPa at the compression level (L3-4) under exion moments, compared with the annulus stress of 1.55 MPa at L3-4 under exion moment in the intact degenerated model. Under exion moments, both the SpinO and ConLa models showed the greatest increase of annulus stress at the decompression level (L3-4) compared with the intact model (Fig. 5). The ConLa model demonstrated a larger annulus stress under flexion moments than were seen in the SpinO model. These patterns of annulus stress were observed in both the healthy and moderate disc degeneration models (Fig. 5). Furthermore, the annulus stress seen in the moderate disc degeneration models was larger than that of matched healthy disc models (Fig. 5). Therefore, the decompression level (L3-4) in the ConLa model with moderate disc degeneration showed the highest

annulus stress.

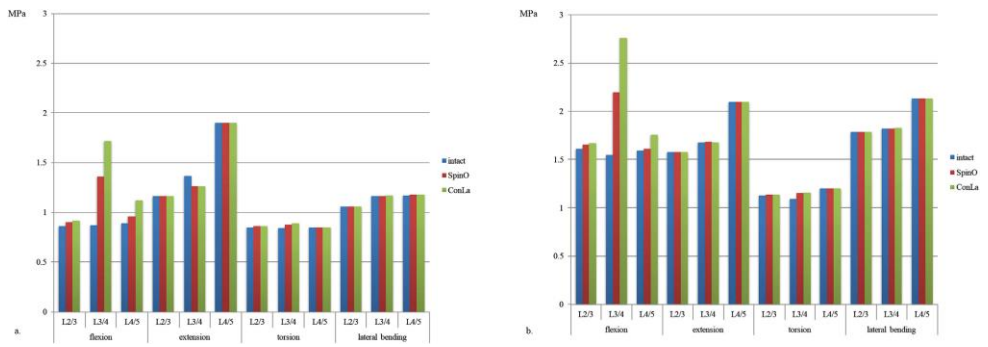

Fig. 5. Maximal von Mises stress in the annulus fibrosus of the intact, spinous process osteotomy, and conventional laminectomy models related to disc degeneration under four moments.

a. Healthy disc models, b. Moderate disc degeneration models.

3.3. Comparison of percent changes of annulus stress from the intact model to the matched decompression model with both healthy and moderately degenerated disc

The largest percent increment of annulus stress (approximately 50%-100%) from the intact model to the matched decompression models

with each SpinO and ConLa technique was noted at the level of decompression (L3-4) under the flexion moment, in both the healthy and moderate disc degeneration models (Fig. 6). The increase in annulus stress shown under the torsion moment was <10%. In addition, the ConLa models always produced a larger increase in annulus stress than the SpinO models, regardless of the disc degeneration state (Fig. 6). However, although annulus stress increased with disc degeneration, the percent change from the intact model to the matched decompression models with each SpinO and ConLa technique was less in the moderate disc degeneration model than in the healthy disc model (Fig. 6). There was a 41.9% and 78.1% increase in annulus stress from the intact model at L3-4 under the flexion moment in the SpinO and ConLa models with moderate disc degeneration, respectively, whereas a 56.3% and 97.4% increase in annulus stress from the intact model was observed at L3-4 under the flexion moment in the SpinO and ConLa models with a healthy disc, respectively (Fig. 6)

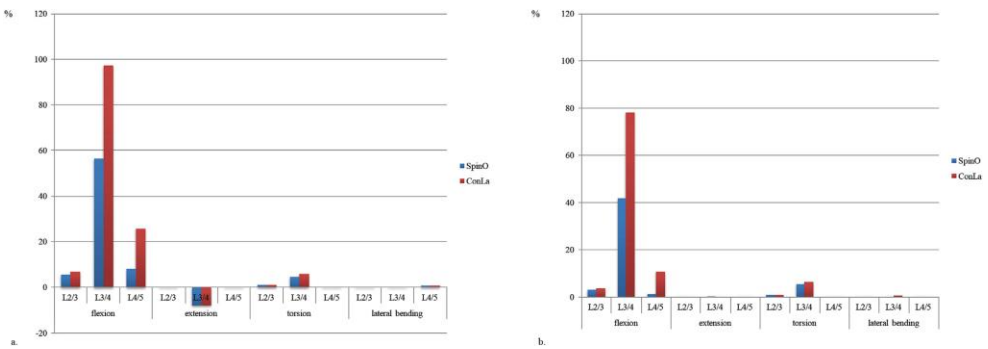

Fig. 6. Percent changes of annulus stress in the intact and decompression models between the healthy and moderate disc degenerative models.

a. Healthy disc models, b. Moderate discdegeneration models.

3.4. Comparison of nucleus pressure in the intact, SpinO, and ConLa models related to disc degeneration

Decompression models with a healthy disc demonstrated a minimal increase of intradiscal pressure (0.55 MPa in the SpinO model and 0.58 MPa in the ConLa model) at the level of decompression (L3-4) under the flexion moment, compared with the intact model (0.54 MPa) with a healthy disc (Fig. 7). However, in the moderate disc degeneration models,

there was a 66.7% (0.15 MPa) and 100% (0.18 MPa) increase in disc pressure in the SpinO and ConLa models, respectively, at the level of decompression (L3-4) under the flexion moment, compared with the intact model (0.09 MPa) with moderate disc degeneration (Fig. 7).

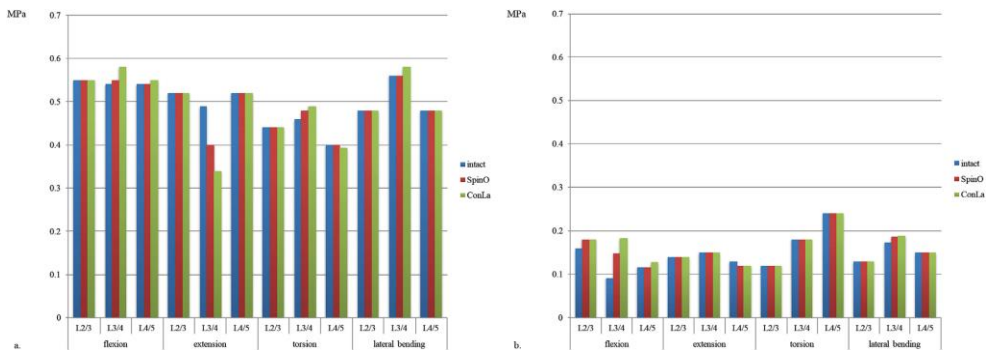

Fig. 7. Nucleus pressure in the intact, spinous process osteotomy, and conventional laminectomy models related to disc degeneration.

a. Healthy disc models, b. Moderate disc degeneration models.

Chapter 4. Discussion

The present study shows that the biomechanical influence of both decompression surgery and disc degeneration occur simultaneously. The ConLa technique almost always led to higher annulus stress than the SpinO technique, both in the healthy disc and moderate disc degeneration models. Between the healthy and moderate degeneration disc models, however, different results were found concerning the percent increment of annular stress, from the intact model to the decompression model. Similar to a previous study on decompression surgery and disc stress[2], the annulus stress at the level of decompression was much higher in the ConLa model than in the SpinO model, especially under flexion and torsion moments. This is attributable to the preservation of PLC in the SpinO model.[2] Furthermore, these results were also seen in both the healthy disc and moderate disc degeneration models. Therefore, the present results suggest that the preservation of the PLC leads to less disc stress at the decompression

level in both healthy patients and in those with moderate disc degeneration. Disc degeneration per se can also influence the biomechanics of the lumbar spine.[22,31,32] Previous studies demonstrated that disc degeneration increases the internal stress on the annulus due to the annulus operating upon compression force rather than tensile force in relation to degenerative remodeling.[31] Likewise, in this study, because annulus stress in itself increased with the corresponding disc degeneration and with laminectomy, the annulus stress at the L3-4 decompression level was the highest under the flexion moment in the ConLa model with moderate disc degeneration. Contrarily, because intradiscal pressure is determined by hydrostatic pressure [33], nucleus pressure is decreased with disc degeneration by the loss of proteoglycan that occurs with the aging process.[34] Interestingly, the comparison of the percent increment from the intact to the decompression models between healthy and moderate disc degeneration showed different findings. The percent change at L3-4

from the intact model to the matched decompression model was less in the moderate disc degeneration model than in the healthy disc model. This means that the degenerative models would be less influenced by the decompression technique. This result is attributed to the stabilizing effect of disc degeneration. In fact, an earlier milestone study by Kirkaldy-Willis and Farfan described an increase in spinal flexibility for mild and moderate degenerative scenarios, defined as instability, and a stiffening only for severe degeneration.[5] Recent works based on an extensive database of in vitro experiments contradicted this concept, thus suggesting that spinal degenerative changes including disc degeneration generally induces a progressive stiffening of the spinal segment.[34,35] Because the moderate disc degeneration model has higher stiffness, the effect of removing the PLC would be alleviated in the moderate disc degeneration models. Therefore, these FE results suggest that the effects of the technique used for decompression surgery would be different based on the state of degeneration of the

lumbar spine. These findings correspond well with those of a previous study that showed that the percent increment of disc stress at the adjacent segment after fusion decreased with disc degeneration of the adjacent segment.[22] The limitations of this study should be acknowledged. First, as shown in a previous FE study[22], simulation for degenerative changes was applied only in the disc height and material properties of the annulus and nucleus. Because the change of material properties of all degenerative spinal ligaments was not known completely, this could not be simulated in the present study. Second, the present study included a model with moderate disc degeneration. Given that degenerative lumbar spinal disease represents a wide spectrum of degeneration, mild or severe disc degeneration should be included in future research. Third, we did not simulate facet degeneration, which might be critical for interpretation of the present results. However, to our knowledge, there has been no study on facet degeneration. Therefore, future research should include FE modeling with simulation of both disc

and facet degeneration. To summarize, the current model represented only a certain degree (moderate) of disc degeneration within the wide spectrum of degeneration with regard to severity and anatomical extent. Therefore, the present results are valid only for the present model. From this perspective, the clinical implication and generalizability of the current results should be cautiously adapted.

Chapter 5. Conclusions

In conclusion, the present study at least highlights the biomechanical impact of degenerative changes of the disc at the decompression segment, in relation to the decompression technique. Although the ConLa model in the moderate disc degeneration simulation showed the highest annulus stress, the degenerative models would be less influenced by the decompression technique.

Bibliography

1. Bresnahan L, Ogden AT, Natarajan RN, Fessler RG. A biomechanical evaluation of graded posterior element removal for treatment of lumbar stenosis: comparison of a minimally invasive approach with two standard laminectomy techniques. Spine (Philadelphia, Pa 1976). 2009;34(1):17-23.
2. Kim HJ, Chun HJ, Kang KT, Lee HM, Chang BS, Lee CK, et al. Finite element analysis for comparison of spinous process osteotomies technique with conventional laminectomy as lumbar decompression procedure. Yonsei medical

journal. 2015;56(1):146-53. Epub 2014/12/17. doi: 10.3349/ymj.2015.56.1.146. PubMed PMID: 25510758; PubMed Central PMCID: PMCPMC4276748.

3. Acaroglu ER, Iatridis JC, Setton LA, Foster RJ, Mow VC, Weidenbaum M. Degeneration and aging affect the tensile behavior of human lumbar anulus fibrosus. Spine (Philadelphia, Pa 1976). 1995;20(24):2690-701.

4. Fujiwara A, Lim TH, An HS, Tanaka N, Jeon CH, Andersson GB, et al. The effect of disc degeneration and facet joint osteoarthritis on the segmental flexibility of the lumbar spine. Spine (Philadelphia, Pa 1976). 2000;25(23):3036-44.

5. Kirkaldy-Willis WH, Farfan HF. Instability of the lumbar spine. Clin Orthop Relat Res. 1982;(165):110-23.

6. Chen CS, Cheng CK, Liu CL, Lo WH. Stress analysis of the disc adjacent to interbody fusion in lumbar spine. Medical engineering & physics. 2001;23(7):483-91.

7. Goel VK, Grauer JN, Patel T, Biyani A, Sairyo K, Vishnubhotla S, et al. Effects of charite artificial disc on the implanted and adjacent spinal segments mechanics using a hybrid testing protocol. Spine (Phila Pa 1976). 2005;30(24):2755-64. Epub 2005/12/24. PubMed PMID: 16371899.

8. Shirazi-Adl SA, Shrivastava SC, Ahmed AM.

Stress analysis of the lumbar disc-body unit in compression. A three-dimensional nonlinear finite element study. Spine. 1984;9(2):120-34.

9. Pintar FA, Yoganandan N, Myers T, Elhagediab A, Sances A. Biomechanical properties of human lumbar spine ligaments. Journal of biomechanics. 1992;25(11):1351-6.

10. Goel VK, Kim YE, Lim TH, Weinstein JN. An analytical investigation of the mechanics of spinal instrumentation. Spine. 1988;13(9):1003-11.

11. Wu HC, Yao RF. Mechanical behavior of the human annulus fibrosus. Journal of biomechanics. 1976;9(1):1-7.

12. Shirazi-Adl A, Ahmed AM, Shrivastava SC. Mechanical response of a lumbar motion segment in axial torque alone and combined with compression. Spine (Phila Pa 1976). 1986;11(9):914-27. Epub 1986/11/01. PubMed PMID: 3824069.

13. Polikeit A, Ferguson SJ, Nolte LP, Orr TE. Factors influencing stresses in the lumbar spine after the insertion of intervertebral cages: finite element analysis. European spine journal : official publication of the European Spine Society, the European Spinal Deformity Society, and the European Section of the Cervical Spine Research Society. 2003;12(4):413-20. Epub

2003/09/05. doi: 10.1007/s00586-002-0505-8. PubMed PMID: 12955610; PubMed Central PMCID: PMCPmc3467788.

14. Schmidt H, Galbusera F, Rohlmann A, Zander T, Wilke H-J. Effect of multilevel lumbar disc arthroplasty on spine kinematics and facet joint loads in flexion and extension: a finite element analysis. European spine journal. 2012;21 Suppl 5:S663-74.

15. Ruberté LM, Natarajan RN, Andersson GB. Influence of single-level lumbar degenerative disc disease on the behavior of the adjacent segments--a finite element model study. Journal of Biomechanics.

2009;42(3):341-8.

16. Benneker LM, Heini PF, Anderson SE, Alini M, Ito K. Correlation of radiographic and MRI parameters to morphological and biochemical assessment of intervertebral disc degeneration. European spine journal. 2005;14(1):27-35.

17. Adams MA, McNally DS, Dolan P. 'Stress' distributions inside intervertebral discs. The effects of age and degeneration. Journal of bone and joint surgery British Volume. 1996;78(6):965-72.

18. Umehara S, Tadano S, Abumi K, Katagiri K, Kaneda K, Ukai T. Effects of degeneration on the elastic modulus distribution in the

lumbar intervertebral disc. Spine (Philadelphia, Pa 1976). 1996;21(7):811-9.

19. Elliott DM, Setton LA. Anisotropic and inhomogeneous tensile behavior of the human anulus fibrosus: experimental measurement and material model predictions. Journal of biomechanical engineering. 2001;123(3):256-63.

20. Weiner BK, Fraser RD, Peterson M. Spinous process osteotomies to facilitate lumbar decompressive surgery. Spine. 1999;24(1):62-6.

21. El Abed K, Barakat M, Ainscow D. Multilevel lumbar spinal stenosis decompression: midterm outcome using a modified hinge

osteotomy technique. Journal of spinal disorders & techniques. 2011;24(6):376-80.

22. Kim HJ, Kang KT, Chun HJ, Lee CK, Chang BS, Yeom JS. The influence of intrinsic disc degeneration of the adjacent segments on its stress distribution after one-level lumbar fusion. European spine journal: official publication of the European Spine Society, the European Spinal Deformity Society, and the European Section of the Cervical Spine Research Society. 2015;24(4):827-37. Epub 2014/07/16. doi: 10.1007/s00586-014-3462-0. PubMed PMID: 25022861.

23. Wilke H, Heuer F, Schmidt H. Prospective

design delineation and subsequent in vitro evaluation of a new posterior dynamic stabilization system. Spine (Philadelphia, Pa 1976). 2009;34(3):255-61.

24. Schilling C, Kruger S, Grupp TM, Duda GN, Blomer W, Rohlmann A. The effect of design parameters of dynamic pedicle screw systems on kinematics and load bearing: an in vitro study. European spine journal : official publication of the European Spine Society, the European Spinal Deformity Society, and the European Section of the Cervical Spine Research Society. 2011;20(2):297-307. Epub 2010/11/27. doi: 10.1007/s00586-010-1620-6. PubMed PMID:

21110209; PubMed Central PMCID: PMC3030714.

25. Wilson DC, Niosi CA, Zhu QA, Oxland TR. Accuracy and repeatability of a new method for measuring facet loads in the lumbar spine. Journal of biomechanics. 2006;39(2):348-53.

26. Hartmann F, Janssen C, Böhm S, Hely H, Rommens PM, Gercek E. Biomechanical effect of graded minimal-invasive decompression procedures on lumbar spinal stability. Archives of orthopaedic and trauma surgery. 2012;132(9):1233-9.

27. Mimura M, Panjabi MM, Oxland TR, Crisco JJ, Yamamoto I, Vasavada A. Disc degeneration

affects the multidirectional flexibility of the lumbar spine. Spine (Philadelphia, Pa 1976). 1994;19(12):1371-80.

28. Rohlmann A, Zander T, Schmidt H, Wilke H, Bergmann G. Analysis of the influence of disc degeneration on the mechanical behaviour of a lumbar motion segment using the finite element method. Journal of biomechanics. 2006;39(13):2484-90.

29. Patwardhan AG, Havey RM, Meade KP, Lee B, Dunlap B. A follower load increases the load-carrying capacity of the lumbar spine in compression. Spine (Philadelphia, Pa 1976). 1999;24(10):1003-9.

30. Renner SM, Natarajan RN, Patwardhan AG,

Havey RM, Voronov LI, Guo BY, et al. Novel model to analyze the effect of a large compressive follower pre-load on range of motions in a lumbar spine. J Biomech. 2007;40(6):1326-32.

31. Massey CJ, van Donkelaar CC, Vresilovic E, Zavaliangos A, Marcolongo M. Effects of aging and degeneration on the human intervertebral disc during the diurnal cycle: a finite element study. Journal of orthopaedic research. 2012;30(1):122-8.

32. Park WM, Kim K, Kim YH. Effects of degenerated intervertebral discs on intersegmental rotations, intradiscal pressures, and facet joint forces of the

whole lumbar spine. Computers in biology and medicine. 2013;43(9):123440. Epub 2013/08/13. doi: 10.1016/j.compbiomed.2013.06.011. PubMed PMID: 23930818.

33. Sato K, Kikuchi S, Yonezawa T. In vivo intradiscal pressure measurement in healthy individuals and in patients with ongoing back problems. Spine. 1999;24(23):2468-74.

34. Galbusera F, Schmidt H, Neidlinger-Wilke C, Wilke H-J. The effect of degenerative morphological changes of the intervertebral disc on the lumbar spine biomechanics: a poroelastic finite element investigation. Computer methods in biomechanics and

biomedical engineering. 2011;14(8):729-39.

35. Galbusera F, Schmidt H, Neidlinger-Wilke C, Gottschalk A, Wilke HJ. The mechanical response of the lumbar spine to different combinations of disc degenerative changes investigated using randomized poroelastic finite element models. European spine journal : official publication of the European Spine Society, the European Spinal Deformity Society, and the European Section of the Cervical Spine Research Society. 2011;20(4):563-71. doi: 10.1007/s00586-010-1586-4. PubMed PMID: 20936308; PubMed Central PMCID: PMC3065610.

국문 초록

배경: 요추 감압술과 퇴행성 변화의 정도가 각각 요추의 생역학에 영향을 미칠 수 있음이 알려져 있으나, 두가지 요소가 동시에 어떤 작용을 하는지는 아직까지는 연구되지 않았다. 본 연구는 지금까지 연구되지 않았던 요추의 퇴행성 변화 정도와 요추 감압술 종류에 따른 수술 후 요추 추간판의 생역학적 변화를 분석하였다.

방법: 본 연구에서는 제2요추부터 제5요추간의 정상 소견 및 퇴행 변화에 대한 유한요소모델을 사용하였다. 본 연구에서는 고식적 후궁절제술 (ConLa) 및 극돌기 절골술(SpinO)을 통해 시행한 제3-4 요추간 감압술을 시행한 두 가지 상이한 요추 감압술에 대한 시나리오를 설정하였으며, 총 6개의 모델을 분석하였다. 예비하중 조건에서 체간의 굴곡, 신전, 외측 굴곡 및 염전에 대해 7.5 Nm 모멘트를 부하하였다. 각각의 모델을 통해 수술 분절 (제3-4 요추간) 및 인접 분절 (제2-3 요추간 및 제 4-5 요추간)의 섬유륜과 수핵 압력의 최대 유효응력 (Von-Mises stress)를 분석하였다.

결과: 고식적 후궁절제술 모델 (ConLa model)과 추간판의 퇴행 모델 (disc degeneration model)은 각각 극돌기 절골술 모델

(SpinO model)과 정상 추간판 모델에 비해서 모든 체간 변화에 따라 수술 분절인 제 3-4 요추간 섬유륜의 응력이 더 크게 나타났다. 중증도의 추간판 퇴행변화를 가정한 고식적 후궁절제술 모델은 수술 분절에서 최대의 섬유륜 응력을 보인다는 것 또한 알게 되었다. 반면 퇴행 모델과 매치된 정상 추간판 모델에서의 제 3-4 요추간 섬유륜 응력의 변화 분율은 정상 추간판 모델에서보다 중증도의 추간판 퇴행 변화 모델에서 더 적게 나타났음을 알 수 있었다.

결론: 비록 중증도의 추간판 퇴행성 변화를 가정한 고식적 후궁절제술 모델이 최대의 섬유륜 응력을 보였으나, 퇴행 모델은 요추 감압술의 영향을 적게 받았다고 할 수 있다.

주요어: 요추, 감압술, 퇴행성 변화, 척추후궁절제술, 극상돌기 절골술, 유한 요소 모델

학번: 2013-30812